Lab on a Chip

Dynamic Article Links

Cite this: *Lab Chip*, 2012, **12**, 4610–4616

www.rsc.org/loc

PAPER

Two-hundredfold volume concentration of dilute cell and particle suspensions using chip integrated multistage acoustophoresis†

Maria Nordin*[a] and Thomas Laurell*[ab]

Received 31st May 2012, Accepted 9th August 2012
DOI: 10.1039/c2lc40629b

Concentrating cells is a frequently performed step in cell biological assays and medical diagnostics. The commonly used centrifuge exhibits limitations when dealing with rare cell events and small sample volumes. Here, we present an acoustophoresis microfluidic chip utilising ultrasound to concentrate particles and cells into a smaller volume. The method is label-free, continuous and independent of suspending fluid, allowing for low cost and minimal preparation of the samples. Sequential concentration regions and two-dimensional acoustic standing wave focusing of cells and particles were found critical to accomplish concentration factors beyond one hundred times. Microparticles (5 μm in diameter) used to characterize the system were concentrated up to 194.2 ± 9.6 times with a recovery of 97.1 ± 4.8%. Red blood cells and prostate cancer cells were concentrated 145.0 ± 5.0 times and 195.7 ± 36.2 times, respectively, with recoveries of 97.2 ± 3.3% and 97.9 ± 18.1%. The data demonstrate that acoustophoresis is an effective technique for continuous flow-based concentration of cells and particles, offering a much needed intermediate step between sorting and detection of rare cell samples in lab-on-a-chip systems.

Introduction

Concentrating rare cells or dilute cell samples is a critical step in bioanalysis and cell biology. Low concentration microorganisms or rare cells associated with various diseases, such as bacteria in bacteraemia[1] or circulating tumour cells[2] often require concentration before detection and identification. This crucial step can mean the difference between a positive or negative diagnostic readout. Assessment of water and food quality[3] can also pose challenges in terms of sample concentration, where contaminating cells often are low in numbers.

Centrifugation is the most widely used method for concentrating samples. However, this technique suffers from drawbacks, especially in combination with low cell numbers or small liquid volumes.[4] Concentration of low cell numbers will require small re-suspension volumes that are not practically possible to handle in ordinary centrifugation systems. Furthermore, centrifugation of low cell numbers will increase the risk of substantial sample losses if the sample forms a pellet that is too small to be seen or if no pellet forms at all. Centrifugation may also have an effect on cell viability[5] and function,[6] which in the end can bias readouts. When combined with lab-on-a-chip applications, where small volumes often are the end product, the centrifuge may not be a suitable option.

Microfluidic-based and lab-on-a-chip concentrating systems provide potential solutions to the problems inherent in the use of centrifugation. Microfluidic systems make it possible to handle samples in a continuous mode, without restricting sample volumes, as large volumes may have to be processed in order to collect a sufficient number of cells from highly dilute samples. As opposed to most macroscale systems, they also offer the possibility of handling samples in a closed environment. This allows for concentration of rare cells for transplantation or cell culture, without exposing them to the same contamination risks as *e.g.* ordinary centrifugation or FACS based cell processing would.

Possibilities for concentration in microfluidic systems have previously been studied. Reported methods include the use of gravity,[4] hydrodynamic forces,[7,8] electrical forces,[9–14] magnetic forces[15] and acoustophoresis-enhanced sedimentation.[16] The results obtained using these methods are summarised in Table 1. It can be seen that there is a lack of systems yielding high concentration factors while maintaining a high recovery and throughput.

This paper presents a high-throughput acoustophoresis microfluidic chip, capable of achieving concentration factors for cells and particles of up to two hundred times with minimal losses. The chip utilises ultrasound standing wave forces to focus cells and particles, in two dimensions, in a confined liquid volume in the micro-channel centre. Cells and particles are focused by the primary acoustic radiation force in two

[a]*Dept. Measurement Technology and Industrial Electrical Engineering, Div. Nanobiotechnology, Lund University, Lund, Sweden. E-mail: maria.nordin@elmat.lth.se*
[b]*Dept. Biomedical Engineering, Dongguk University, Seoul, South Korea. E-mail: thomas.laurell@elmat.lth.se*
† Electronic supplementary information (ESI) available. See DOI: 10.1039/c2lc40629b

Table 1 Summary of primary results obtained on concentration in microfluidic systems

Method	Particle/cell	Initial concentration (mL^{-1})	Sample inflow rate ($\mu L\ min^{-1}$)	Concentration factor	Recovery/ Efficiency (%)	Comment	Reference
Gravity	LNCaP	$5*10^5$	Max 8	9.7	98.9 ± 0.2		4
Microvortices	MCF-7	250	4400	20	20		7
Hydrodynamic	1–3 μm polymer bead	$1.8*10^7$, $4.7*10^6$ and $6.8*10^6$, respectively	0.5	63–80	67–90		8
Electrostatic trapping	*Salmonella*	10^6 CFU	100	14.2	85.2		9
Zone electrophoresis Isoelectric focusing	*E. herbicola*	NA	4.98	NA	NA	Needs specific buffer	10
Dielectrophoretic trapping	HeLa	$5*10^5$	0	NA	76	Needs specific buffer	11
Ion concentration polarization	RBC *E. coli*	200–500 times dilute of whole blood	Max 5	19 and 20, respectively	100	Needs specific buffer	12
Dielectrophoretic trapping	*E. coli* *S. Cerevisiae*	$6*10^8$ $6*10^6$	NA	88.1 and 23.14, respectively (in the trap)	NA	Needs specific buffer	13
Free flow electrophoresis	*E. coli*	$5*10^4$ CFU	15	53.57	87.06	Needs specific buffer	14
Immunomagnetic trapping	*E. coli*	$1*10^3$	200[a]	NA	82	Needs antibody-labeled magnetic beads	15
Acoustophoresis-enchanced sedimentation	*S. cerevisiae*	$7.2*10^9$	4800	5	98.5		16

[a] The input flow rate is not given, but rather the total flow rate of sample solution and capture solution.

dimensions, according to their intrinsic properties size, density and compressibility.[17–22] Acoustophoresis is a label-free method, allowing for low cost and minimal sample preparation. In addition, the ultrasound has previously been shown to be gentle to cells.[23–26] The continuous flow mode makes it possible to achieve concentration factors of several orders of magnitude of dilute samples, and the method can be used independently of suspending fluid. Furthermore, the continuous flow processing makes it suitable for integration with downstream unit operations, providing a much needed intermediate step, *e.g.* between sorting and detection of rare cell samples in microfluidic chips.

Material and methods

Microfabrication

The silicon chip was fabricated using photolithography and anisotropic wet etching in KOH (40 g/100 mL H_20, 80 °C). Holes for inlets and outlets were drilled in the silicon using a diamond drill. The chip was sealed by anodic bonding of a glass lid. For more detail on the chip fabrication see.[20]

Device design

The chip was composed of one inlet and one or two trifurcation outlet regions connected by a straight channel allowing cells and particles to become acoustically focused between each outlet region (Fig. 1). The focusing channel was 375 μm wide and 160 μm deep and the channel lengths between each outlet region were 30 and 5 mm, respectively. The channel width and height corresponded to half a wavelength of ultrasound at 1.99 MHz and 4.68 MHz. The chip was actuated using piezoceramic transducers (PZ26, Ferroperm piezoceramics, Kvistgaard, Denmark) resonant at 2 MHz and 5 MHz. The 2 MHz piezo was attached by cyanoacrylate glue (Loctite Super glue, Henkel Norden AB, Stockholm, Sweden) to the glass lid covering the entire length and a third of the width of the chip. The 5 MHz piezo was attached to the silicon back of the chip covering the space between the inlet and the first outlet region. In order to keep settings identical in the experiments with one and two trifurcated outlet regions, the same chip was used for both configurations. In the one outlet region configuration the unused outlets on the chip were sealed (Fig. 1a).

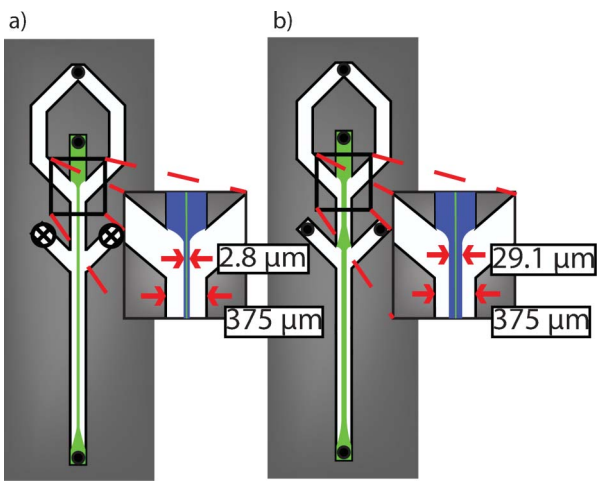

Fig. 1 Chip configurations. a) The one outlet region system. The unused, sealed outlets are indicated by a black cross. b) The two outlet regions system. The green lines illustrate particles focusing in the channel. In the two outlet regions system the particles will have to re-focus after the first outlet region. The insert drawings illustrate the maximum allowed width of the critical centre fraction of the input flow (blue) that must contain the focused particles for these to all be collected in the centre outlet. Insert numbers indicate the minimum allowed width of this fraction when doing 100 times concentration in both systems. The total channel width, 375 μm is also indicated.

Instrumental setup

The two transducers were actuated using power amplifiers (width actuation: Amplifier Research 75A250A, Souderton, PA, USA; depth actuation: an in-house built circuit board with a power amplifier: LT1012, Linear Technology Corp., Milpitas, CA, USA). Two function generators (Agilent 33120A, Agilent technologies Inc. Santa Clara, CA, USA) were used. The applied voltage was monitored using an oscilloscope (TDS 210, Tektronix, UK Ltd., Bracknell, UK). Microscopy pictures and videos were generated using a Dino-Lite digital microscope (AM413T5 Dino-Lite Pro, AnMo Electronics Corporation, Hsinchu, Taiwan).

Experimental setup

The flow rates in the chip were controlled by connecting all the inlets and outlets to glass syringes (Hamilton Bonaduz AG, Bonaduz, Switzerland) mounted on syringe pumps (Nemesys, Cetoni GmbH, Korbussen, Germany). The inflow rate was, unless otherwise stated, set to 100 μL min^{-1} and the centre output flow rates were varied between 1–20 μL min^{-1} to achieve different concentration factors. An overview of the combined flow rate settings along with the results can be found in Supplementary Table 1–3. Samples were collected using a 2-position 3-port valve (MV201-C360, LabSmith, Livermore, CA, USA) connected in series with the last centre outlet. The sample collection system is illustrated in more detail in Supplementary Fig. 2. The collected 10 μL sample volumes were subsequently diluted to an appropriate volume, and counted in a Bürker chamber (Marienfeld, Lauda-Königshofen, Germany). To minimise possible measurement errors from sedimentation in the syringes, concentration factors were obtained by comparing samples collected with the ultrasound either on or off. The recovery values were obtained as the ratio between measured particle concentration and theoretical concentration at 100% recovery.

Microparticles

For characterizing the system, polystyrene particles (5 μm in diameter) (Fluka/Sigma-Aldrich, Buchs, Switzerland) were suspended in MilliQ H_2O and 0.002% Triton-X100 to a particle concentration of 0.02 wt% or 0.005 wt%. Particle and cell concentrations were deliberately kept relatively high, in terms of rare cells, to facilitate enumeration in the analytical step.

Confocal microscopy

Confocal microscopy was used to depict the distribution of microparticles when performing one- and two-dimensional focusing. Yellow fluorescent particles (4.1 μm in diameter) (Kisker GmbH, Steinfurt, Germany), suspended in MilliQ H_2O to a concentration of $1*10^6$ mL^{-1}, were used to obtain confocal images with an Olympus microscope (BX51WI, Olympus Corporation, Tokyo, Japan) and the Fluoview 300 software was subsequently used to reconstruct cross section images.

Red blood cells

Red blood cells were used as a model cell to further characterize the system. Blood samples were obtained from healthy volunteers at Lund University Hospital (Lund, Sweden). Whole blood was diluted 5000 times in PBS prior to concentration experiments.

Prostate cancer cells

The human prostate cancer cell line, DU145, was used as a model of circulating tumour cells. The cells were obtained from the American Type Tissue Collection and cultured according to their recommendations. Briefly, RPMI-1640 medium (Sigma-Aldrich, St Louis, MO, USA) was supplemented with 10% fetal bovine serum (Sigma-Aldrich, St Louis, MO, USA), 55 IU mL^{-1} penicillin and 55 μg mL^{-1} streptomycin (Sigma-Aldrich, St Louis, MO, USA). Cells were cultured at 37 °C in a humidified atmosphere containing 5% CO_2. $1*10^6$ cells mL^{-1} were used to

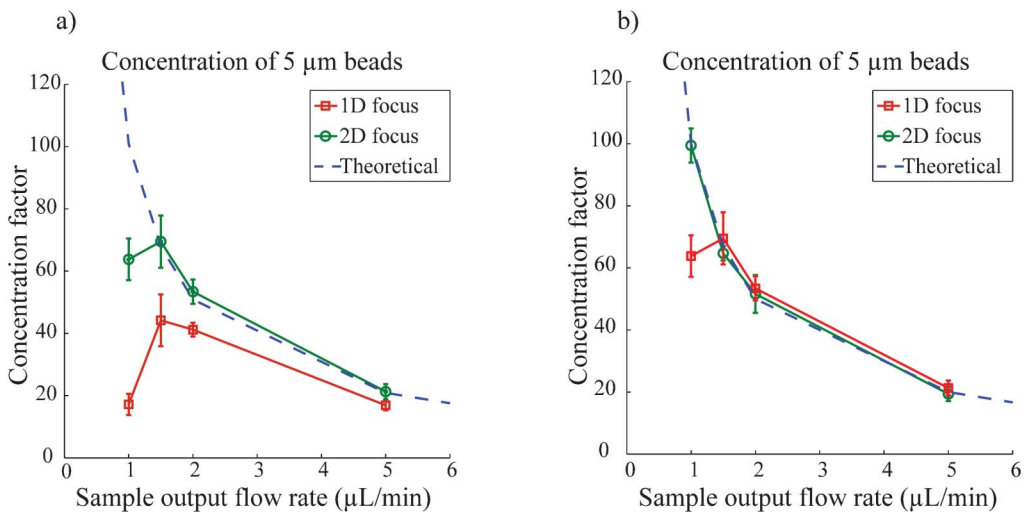

Fig. 2 Concentration of 5 μm diameter polystyrene particles for different sample output flow rates. a) Concentration using one trifurcation outlet region. b) Concentration using two trifurcation outlet regions. The error bars show the standard deviation, n = 3 (3 control and 3 concentrated samples). The input flow rate was maintained constant at 100 μL min^{-1}. The dashed line indicates the theoretical concentration factor at 100% recovery.

obtain the "ultrasound off" control samples. In the experiments assessing 100 and 200 times concentration, the cell input suspensions were diluted to $1*10^5$ cells mL^{-1} and $2.5*10^4$ cells mL^{-1}, respectively.

Results and discussion

In this paper we report on an acoustophoresis chip for several orders of magnitude concentration of cells and particles. The chip operates in a half wave length resonance mode and utilises ultrasonic standing wave forces, in two dimensions, to focus particles and cells in the acoustic pressure node located in the micro-channel centre.

Chip characterization

One-dimensional focusing. First, the concentration capacity using one trifurcation outlet region (Fig. 1a) was investigated, a design extensively used for acoustophoresis.[27] This set-up could concentrate 4.6 $\pm$ 1.1 and 9.0 $\pm$ 2.0 times with a recovery of 92 $\pm$ 22% and 90 $\pm$ 20%, respectively. However, when trying to achieve higher concentration factors, the recovery decreased rapidly. The highest concentration factor for this configuration, 44 $\pm$ 8.3 times with a recovery of 66 $\pm$ 12.4%, was obtained when trying to achieve a concentrate factor of 67 times. This corresponded to a sample output flow rate of 1.5 $\mu L\ min^{-1}$ using a sample input flow rate of 100 $\mu L\ min^{-1}$. When trying to concentrate 100 times, *i.e.* lowering the sample output flow rate to 1 $\mu L\ min^{-1}$, a concentration factor of only 17.2 $\pm$ 3.4 was obtained, resulting in the corresponding recovery of 17.2 $\pm$ 3.4% (Fig. 2a).

There are two causes of the moderate performance of this set-up. The first is explained by the accuracy of the flow system. When trying to achieve high concentration factors, only a minute fraction of the total flow, containing all the particles, should be extracted *via* the centre outlet (*e.g.* 1% of the total flow for 100 times concentration). Given the Poiseuille flow profile, the width of this critical centre fraction that account for 1% of the total flow, is significantly smaller than 1% of the channel width, *i.e.* calculated to be 2.8 μm, when accounting for both the horizontal and the vertical contribution to the flow profile (Fig. 1.).

For the particles to enter the centre outlet they have to be focused within the critical centre fraction of the flow. The 5 μm diameter particles used are larger than the 2.8 μm critical centre fraction width, and consequently, a full recovery of particles under this condition was difficult to achieve. Not only would particles situated side by side in the channel be lost, but minor fluctuations in the flow moving the particle only about half a radius, 1.4 μm, to either side, would also contribute to reduced recovery. Likewise, when the critical centre fraction width was 5.7 μm wide, corresponding to 2% of the total flow, minor flow fluctuations would also have a large impact on the recovery. This partly explains the significantly reduced recovery seen for sample output flow rates between 1 and 2 $\mu L\ min^{-1}$, corresponding to 1 and 2% of the total flow using a total flow rate of 100 $\mu L\ min^{-1}$ (Fig. 2a).

The second cause of the moderate performance, when trying to generate higher concentration factors, is found in a combination of the ultrasonic standing wave conditions and the flow system. In the outlet region, where the channel widens and the width no longer matches a single node ultrasound standing wave, an undefined acoustic field of undesired higher modes, not located in the channel centre, is present. As most of the particles pass in the rapid flow regime, there will not be sufficient time for the particles to be deflected from their original trajectory. However, particles positioned close to the top and bottom of the channel, where the flow velocity approaches zero, will spend much longer time in this undefined acoustic field and may thus be deflected from their original trajectory (Fig. 3a). Since the width of the critical centre fraction that exits through the centre outlet is narrow, a lateral displacement of a few micrometers will mean the difference between particles entering the centre outlet or escaping to the waste side outlets. Increasing the acoustic amplitude of the one-dimensional horizontal acoustic focus will not narrow the focused band further to allow the slow-moving particles to enter the centre outlet. In fact, this will counteract the purpose and rather increase the forces in the undefined acoustic field in the outlet region, causing even more particles to escape to the side outlets. The influence of the undesired standing wave node patterns in the outlet region is demonstrated in Fig. 4 and supplementary video 1, where the actuation amplitude was increased to emphasize the outlet region artefact. The undefined acoustic field separates the focused particles in several bands located at different channel depths. Particles closer to the top and bottom of the channel tend to escape to the sides and will eventually, with increased amplitude, also get temporarily trapped in local vortex-surrounded hot spots.

Two-dimensional focusing. The lateral particle migration caused by the undefined acoustic field in the outlet region can be prevented by applying a second vertical standing wave, orthogonal to the first one, resonating in the main focusing channel as well as the outlet regions. This will focus the particles in two dimensions. The two-dimensional focusing will position the particles in the faster moving flow regime in the channel centre (Fig. 3d), decreasing their retention time in the undefined acoustic field at the outlet region, and hence their lateral migration (Fig. 3b) (A comparison between one-dimensional and two-dimensional focusing can be seen in Fig. 3 and supplementary video 2.). With two-dimensional focusing, higher concentration factors could be achieved, and a concentration factor of 69 $\pm$ 8.4 times with the corresponding recovery of 103 $\pm$ 12.1% was obtained (Fig. 2a). However, it was still not possible to achieve a concentration factor of 100 times, as the critical centre fraction was too narrow to contain all the particles within the required 2.8 μm wide zone. The recovery values were obtained as the ratio between measured particle concentration and theoretical concentration at 100% recovery. Hence, a combination of a measurement inaccuracy and the fact that the concentration factors are dependent on an exact flow rate may yield mean recovery values above 100%.

Multiple outlet regions. In the single outlet region set-up, it is clear that the width of the critical centre fraction is the limiting factor for achieving high concentration factors. Collecting the sample from a wider centre fraction would, on the other hand, mean a lower concentration factor. A solution to this dilemma is to realise a system utilising sequential outlet regions, allowing a

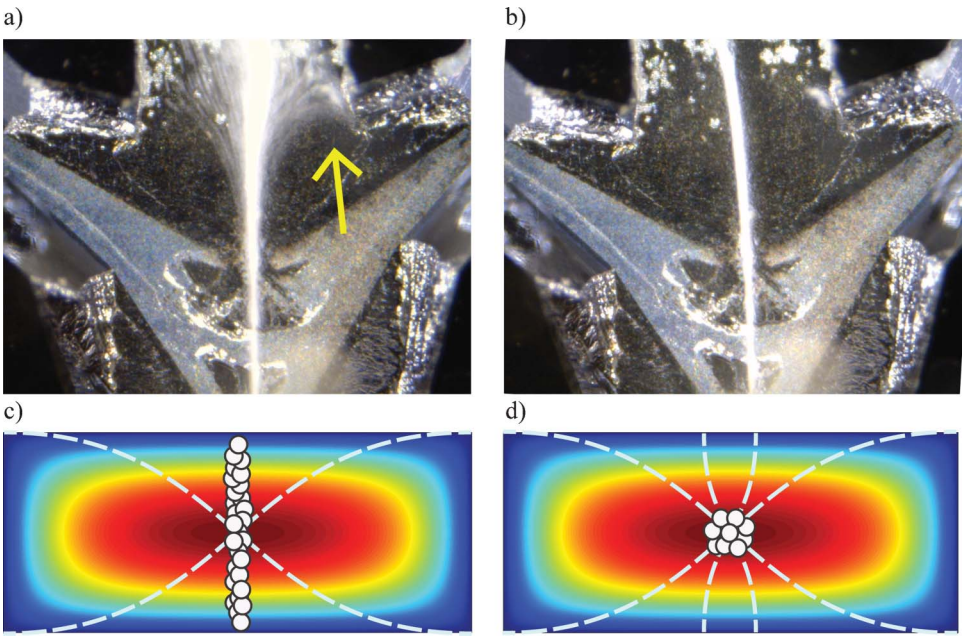

Fig. 3 a) Particles focused in one dimension in the last outlet region. The yellow arrow indicates escape of particles to the side outlet. b) Particles focused in two dimensions in the last outlet region. No escape of particles occurs. c) Schematic cross-section of the micro-channel showing particles focused in one dimension and their position within the Poiseuille flow profile. Red represents the fastest and blue the slowest moving fluid regime. The dashed lines indicate the ultrasound standing wave. d) Cross-section of the micro-channel showing particles focused in two dimensions and their position within the Poiseuille flow profile.

lower split flow rate ratio in each step. Although, each step only generates moderate concentration factors, in the end they will multiply to higher concentration factors. Importantly, the wider fluid fraction collected in the centre outlet allows for larger particle deviations from the original central flow trajectory, and hence a lower loss of cells or particles is ensured. For this reason a set-up with two sequential outlet regions was further studied.

Using the set-up with two sequential outlet regions substantially increased the obtainable concentration factors as predicted. The performances of both the one-dimensional and two-dimensional focusing systems displayed significant improvements. Using one-dimensional focusing and two outlet regions, a concentration factor of 67.4 ± 6.2 was obtained with a recovery of 100.6 ± 9.3% (Fig. 2b). The attempts of doing 100 times sample concentration resulted in a concentration factor of 52.7 ± 4.3 and a recovery of 52.7 ± 4.3%.

By using two-dimensional focusing in the multiple-outlet set-up, however, a sample concentration of 99.4 ± 5.5 times was accomplished with the corresponding recovery of 99.4 ± 5.5%. Based on these findings, the two-dimensional focusing system using two outlet regions was further investigated, and concentration factors up to 194.2 ± 9.6 times with a recovery of 97.1 ± 4.8% were obtained (Table 2).

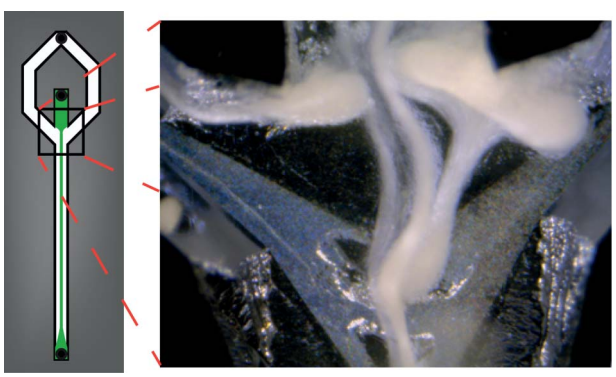

Fig. 4 The effect of the undesired standing wave node pattern, in the last outlet region, on particles focused in one dimension. The acoustic field separates the focused particle-band into several bands located at different channel depths, where the particles moving closer to the bottom and top of the channel become diverted to the side outlets or temporarily trapped in local hot spots surrounded by vortices.

Confocal microscopy

To demonstrate the effect of the two-dimensional acoustic focusing, confocal microscopy was used. The difference in one- and two-dimensional focusing can clearly be seen in Fig. 5. The magnification was limited to x20 in order to allow imaging of the entire channel cross section. This resulted in a confocal depth of

Table 2 Concentration of RBCs, DU145 and 5 μm diameter particles. Sample output flow rate was maintained constant at 1 μL min^{-1}. Errors indicate the standard deviation for n = 3 (3 control and 3 concentrated samples)

	Sample inflow rate (μL min^{-1})	Concentration factor	Recovery (%)
Red blood cells	100	100.7 ± 5.3	100.7 ± 5.3
	150	145.8 ± 5	97.2 ± 3.3
	200	181.1 ± 22.8	90.7 ± 11.4
DU145	100	98.9 ± 3.1	98.9 ± 3.1
	200	195.7 ± 36.2	97.9 ± 18.1
5 μm beads	200	194.2 ± 9.6	97.1 ± 4.8

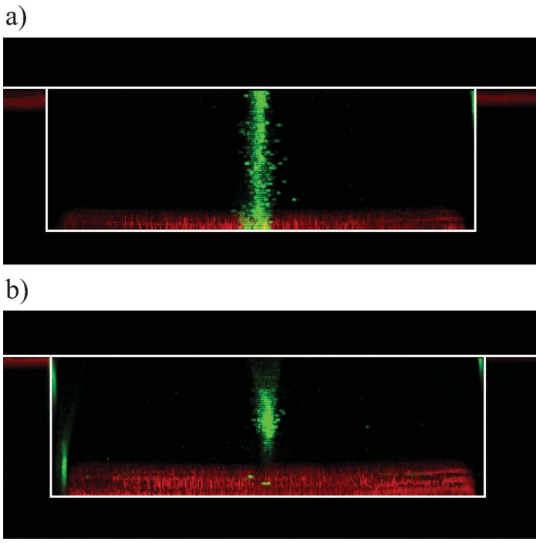

Fig. 5 Confocal images showing a cross-section of the micro-channel as indicated by the white square. a). Particles focused (green) in one dimension vertically. The channel bottom is viewed in red. b). Particles focused in two dimensions. The focused cluster appears longer in the height direction because of the confocal depth. This is illustrated by the elongated image of a stationary particle in the lower left corner of the flow channel. The confocal depth was about 20 μm.

about 20 μm, hence causing features in the images to appear longer, mostly in the vertical direction of the channel.[28] Consequently, the two-dimensionally focused particle cluster appeared more elongated than round (Fig. 5b and further illustrated in supplementary Fig. 1).

Red blood cell concentration

Highly diluted human red blood cells (RBCs) were used as a model system to study the abilities to concentrate live cells. A concentration factor of 145.8 ± 5.0 times with a recovery of 97.2 ± 3.3% (Table 2) was achieved when increasing the sample input flow rate to 150 μL min^{-1}, maintaining the sample output flow rate constant at 1 μL min^{-1}. Attempts to reach a concentration factor of 200 times by increasing the input flow rate to 200 μL min^{-1}, and maintaining the sample output flow rate of 1 μL min^{-1}, resulted in a reduced cell recovery of 90.7 ± 11.4% and a corresponding concentration factor of 181.1 ± 22.8. The reason for the increased loss of cells was visually confirmed to be attributed to an insufficient primary radiation force in the height direction of the channel. The reduced retention time in the channel caused by the increased total flow rate did thereby not allow all cells to focus vertically into the central acoustic pressure node, and thus some of the cells escaped to the side outlets in the region of the undefined acoustic field.

Prostate cancer cell concentration

The cell concentrator chip is intended for rare cell concentration, *e.g.* circulating tumour cells, as a step prior to on-chip analysis or cell culture. A prostate cancer cell line, DU145, was used as a model of circulating tumour cells. A maximum concentration factor of 195.7 ± 36.2 times with a recovery of 97.9 ± 18.1% was obtained (Table 2). The relatively large variations in these experiments were due to variations in the reference samples. Although relatively high concentration factors have been achieved with minute losses, the outlined cell concentrating strategy holds promise for further improvements.

Increasing the input flow rate and maintaining the sample output flow rate constant yields higher concentration factors. The current flow system is, however, limited by a difficulty in balancing a flow in the central outlet that is smaller than 0.5% of the total flow rate. Nevertheless, it can be anticipated that a fully integrated microfluidic solution will display improved performance, by a reduction in flow imbalance disturbances, which the current set-up with chip tubing connections to sample loops and syringe pumps may induce.

When using a 2 MHz transducer particles smaller than about 2 μm in diameter (density like polystyrene or cells) focus very slowly. Efficient focusing at smaller particle size is counteracted by acoustic streaming.[29] Smaller particles can, however, be focused by using *e.g.* a higher actuation frequency. Using the proposed chip design together with at higher frequency smaller cells or particles could be concentrated as well. A higher frequency will require a narrower channel width to satisfy the half wave length standing wave criteria and hence a decreased channel cross section. This in turn yields a shortened retention time in the acoustic focusing zone when operating at unchanged flow rates. We currently don't know if unchanged flow rates could be used in combination with a channel that is designed for a higher frequency and yet obtain efficient concentration factors for smaller species such as bacteria.

The variability of performance between devices is experienced to be low. However, no particular study in this respect has been performed. The only foreseen variability is minute variations in the optimal actuation frequency caused by small variations in channel width and height between fabrication batches and different particles suspension fluids.

Conclusions

This paper explores the use of acoustophoresis to concentrate dilute cell samples and particles. It is shown that two-dimensional acoustic standing wave focusing outperforms one-dimensional focusing and that the strategy of implementing several acoustic focusing regions and sequentially remove excess fluid opens the route to concentration factors in continuous flow mode beyond 100 times. Under high-throughput conditions up to 200 times of volume concentration with a minute loss of cells and particles was accomplished. On-going work will aim at further improved concentration factors and offer means to concentrate rare cell and small volume samples where regular centrifugation does not provide a satisfactory solution. The cell concentrator is currently developed to become an integral part of chip integrated cell separation and analysis units.

Acknowledgements

We thank Dr Per Augustsson for helpful discussions and Dr Cecilia Magnusson for the generous gift of the DU145 cells. The work was supported by the Swedish governmental agency for innovation systems, VINNOVA, CellCARE, grant no. 2009-00236, the Swedish Research Council, grant no.: 621-2010-4389, the Royal Physiographic Society, the Crafoord Foundation and the Carl Trygger Foundation.

References

1 S. Shafazand, *Chest*, 2002, **122**, 1727–1736.
2 W. J. Allard, J. Matera, M. C. Miller, M. Repollet, M. C. Connelly, C. Rao, A. G. J. Tibbe, J. W. Uhr and L. W. M. M. Terstappen, *Clin. Cancer Res.*, 2004, **10**, 6897–904.
3 K. A. Stevens and L.-A. Jaykus, *Crit. Rev. Microbiol.*, 2004, **30**, 7–24.
4 J. Warrick, B. Casavant, M. Frisk and D. Beebe, *Anal. Chem.*, 2010, **82**, 8320–6.
5 D. I. C. Wang, T. J. Sinskey, R. E. Gerner and R. P. De Filippi, *Biotechnol. Bioeng.*, 1968, **10**, 641–649.
6 J. Yang, W. C. Hooper, D. J. Phillips, M. L. Tondella and D. F. Talkington, *Clin. Vaccine Immunol.*, 2002, **9**, 1142–1143.
7 A. J. Mach, J. H. Kim, A. Arshi, S. C. Hur and D. DiCarlo, *Lab Chip*, 2011, **11**, 2827–3016.
8 M. Yamada and M. Seki, *Anal. Chem.*, 2006, **78**, 1357–1362.
9 A. K. Balasubramanian, K. a Soni, A. Beskok and S. D. Pillai, *Lab Chip*, 2007, **7**, 1315–21.
10 C. R. Cabrera and P. Yager, *Electrophoresis*, 2001, **22**, 355–62.
11 C.-P. Jen and H.-H. Chang, *Biomicrofluidics*, 2011, 5.
12 R. Kwak, S. J. Kim and J. Han, *Anal. Chem.*, 2011, **83**, 7348–55.
13 H. Moncada-Hernández and B. H. Lapizco-Encinas, *Anal. Bioanal. Chem.*, 2010, **396**, 1805–16.
14 D. Puchberger-Enengl, S. Podszun, H. Heinz, C. Hermann, P. Vulto and G. a. Urban, *Biomicrofluidics*, 2011, **5**, 44111.
15 P. Grodzinski, J. Yang, R. Liu and M. D. Ward, *Biomed. Microdevices*, 2003, **5**, 303–310.
16 J. J. Hawkes and W. T. Coakley, *Enzyme Microb. Technol.*, 1996, **19**, 57–62.
17 G. R. Goddard, J. C. Martin, S. W. Graves and G. Kaduchak, *Cytometry, Part A*, 2006, **69A**, 66–74.
18 J. J. Hawkes and W. T. Coakley, *Sens. Actuators, B*, 2001, **75**, 213–222.
19 O. Manneberg, J. Svennebring, H. M. Hertz and M. Wiklund, *J. Micromech. Microeng.*, 2008, **18**, 095025.
20 A. Nilsson, F. Petersson, H. Jönsson and T. Laurell, *Lab Chip*, 2004, **4**, 131–5.
21 F. Petersson, L. B. Åberg, A.-M. K. Swärd-Nilsson and T. Laurell, *Anal. Chem.*, 2007, **79**, 5117–23.
22 C. Grenvall, M. Carlsson, P. Augustsson and F. Petersson and T. Laurell, in *Proceedings of μTAS 2007*, ed. J.-L. Viovy, P. Tabeling, S. Cescroix, and L. Malaquin, Paris, 2007, pp. 1813–1815.
23 J. Hultström, O. Manneberg, K. Dopf, H. M. Hertz, H. Brismar and M. Wiklund, *Ultrasound Med. Biol.*, 2007, **33**, 145–51.
24 M. Evander, L. Johansson, T. Lilliehorn, J. Piskur, M. Lindvall, S. Johansson, M. Almqvist, T. Laurell and J. Nilsson, *Anal. Chem.*, 2007, **79**, 2984–2991.
25 J. Dykes, A. Lenshof, I.-B. Åstrand-Grundström, T. Laurell and S. Scheding, *PLoS One*, 2011, **6**, e23074.
26 M. Wiklund, *Lab Chip*, 2012, **12**, 2018–2028.
27 T. Laurell, F. Petersson and A. Nilsson, *Chem. Soc. Rev.*, 2007, **36**, 492–506.
28 R. W. Cole, T. Jinadasa and C. M. Brown, *Nat. Protoc.*, 2011, **6**, 1929–41.
29 P. Augustsson and T. Laurell, *Lab Chip*, 2012, **12**, 1742–1752.